Electronic Supplementary Material (ESI) for Journal of Materials Chemistry A.

Supporting Information

Self-driven membrane filtration by core-shell polymer composites

Zeou Dou,[1] Ting Wang,[1] Wensi Chen,[1] Beichen Lin,[1] Hai Dong,[2] Wei Sun,[2] and Xing Xie[1]*

[1]School of Civil and Environmental Engineering, Georgia Institute of Technology, Atlanta, GA, USA.

[2]Tissue Mechanics Laboratory, The Wallace H. Coulter Department of Biomedical Engineering, Georgia Institute of Technology and Emory University, Atlanta, GA, USA.

[*]E-mail: xing.xie@ce.gatech.edu

S1. Materials and methods

S1.1 Chemicals and materials

Acrylic acid (AA), acrylamide (AM), tetrachloroethylene, toluene, ammonium persulfate (APS), *N,N′*-Methylenebisacrylamide (MBA), NaOH, ethanol (99.5%), *m*-phenylenediamine (MPD), trimesoyl chloride (TMC), and hexane were purchased from Sigma-Aldrich. Commercial maize bran (MB) without processing was purchased from supermarket. Polydimethylsiloxane (PDMS) (Sylgard 184, Dow Chemical Co.).

S1.2 Characterization methods

The thickness and roughness of the PA shells and flat membranes were measured by an atomic force microscope (AFM) (Veeco Dimension 3100). The morphology and surface features were observed by a scanning electron microscope (SEM) (Hitachi 8230) under 5 kV accelerating voltage and a transmission electron microscope (TEM) (Hitachi HT7700) under 120 kV accelerating voltage. The SEM samples were sputter coated with gold before characterization. In the swelling behaviour study, wrinkle-fold evolution of the membrane was observed by an environmental SEM (ESEM) (Hitachi S-3700N) under 14 kV and 100 Pa. Elemental composition was measured by x-ray photoelectron spectrometer (XPS) (Thermo K-Alpha) equipped with an Ar ion sputter gun. Aluminum K-Alpha 1.486 KeV is used as the photoelectron source. The cracking test of the PA shells was conducted under an optical microscope (Zeiss Axio observer 7). The Young's modulus of the Polydimethylsiloxane (PDMS) substrate for the wrinkling test was measured by a universal test machine (Testresources 100 series).

S2. Supplementary text

S2.1 Preparation of the core-shell polymer composites (CSPCs)

The hydrogel core of the CSPC was synthesized through suspension radical polymerization [1]. A certain amount of AA was neutralized in an ice bath with 250 $g \cdot l^{-1}$ NaOH solution to achieve 85% neutralization. Certain amount of AM as the co-monomer, APS as the initiator, and MBA as the crosslinker were added to 12 ml of neutralized AA solution. The mass ratio of AA, AM, APS, and MBA was 100:40:0.84:0.112, respectively. After sonicating for 5 min, a well-mixed ready-to-polymerize monomer solution was obtained. To create a suspension phase for the polymerization, 5 ml tetrachloroethylene was added first into a 20 ml beaker as the bottom layer and 5 ml of toluene was added slowly without mixing as a top layer. The monomer solution was subsequently added into the layered organic phase dropwise (7 µl per drop) to form dispersed individual spheres suspended in the system. During the polymerization at 68ºC, a density gradient formed at the layer interface through spontaneous diffusion and heating turbulence to keep the spheres suspended along the polymerization (**Figure S1**). After reacting for 30 min, the solidified spheres sank to the bottom for collection. The as-prepared spheres were stored in ethanol before use.

The PA shell wrapping the core was synthesized through interfacial polymerization [2]. The spheres were first immersed in aqueous MPD solutions of different concentrations (2, 1, 0.5, or 0.1 wt% in DI water), respectively, for 1 hour to reach a final diameter of ~10 mm. The organic suspension phase consisting of well mixed tetrachloroethylene (~37 vol%) and hexane (~63 vol%) had a density close to that of the hydrogel spheres. Because the density of the hydrogel spheres was fixed, no density gradient was needed. The mixed organic phase contained

different concentrations of TMC (0.06, 0.03, 0.015, or 0.003 wt%). The swollen hydrogel sphere was suspended in the as-prepared organic phase for 2 min, after which, the organic solution was replaced with a 2 M KCl aqueous solution to shrink and store the as-prepared CSPCs before use. The equilibrium diameter of the CSPCs in the 2 M KCl solution was ~3 mm (**Figure S2**). The MB-PAA based CSPCs were synthesized using the same procedure except that the AM was replaced by the same mass of MB.

S2.2 Preparation of PA shell samples for characterization

To investigate the physical and chemical properties of as-prepared PA shells, the shell was separated from the spherical core and transferred onto silicon wafers following a special procedure (**Figure S3**). For characterization only, the integrity of the shell was put aside. Before coating, the sphere was fixed onto a needle for easy handling. After the interfacial polymerization, the CSPC was cut into hemispheres by a razor. The hemispheres were immersed into water at an angle to separate and float the shell. Eventually, the shell was transferred onto a silicon wafer for atomic force microscopy (AFM), scanning electron microscopy (SEM), and x-ray photoelectron spectroscopy (XPS) characterizations. The free-floating shells were also transferred onto copper grids for transmission electron microscopy (TEM) observation.

S2.3 Preparation of the flat-sheet hydrogel-based PA membranes

An aliquot of 1 ml as-prepared monomer solution (see S2.1) was cast onto a glass slide to form a flat layer, and the slide was placed on a hot plate set at 68ºC for 30 min to allow the polymerization. The flat-sheet polymer was then immersed in MPD aqueous solutions of different concentrations (2, 1, 0.5, or 0.1 wt% in DI water), respectively. After swelling for 1 hour, the curved up hydrogel sheet was cut into flat strips for membrane coating in hexane organic phase containing 0.1, 0.05, 0.025, or 0.005 wt% TMC. The interfacial polymerization lasted 2 min. The as-prepared flat-sheet hydrogel PA membrane composite was immersed into DI water at an entering angle to separate and float the membrane for transferring onto PDMS substrates for mechanical property tests.

S2.4 Thickness of the PA shells

The PA shell synthesized on the spherical hydrogel surface was transferred onto silicon wafers as described above for thickness and surface morphology measurements. The height difference from the shell surface to the silicon wafer surface was estimated by the height profile across the shell edge to quantify the thickness (**Figure S4**). AFM results are summarized in table S1. Although the thickness of the relatively smooth PA shells is well presented (**Figures S4A and B**), the thickness estimation for highly crumpled and rough shells can only be accounted as the apparent thickness representing the thickness of the whole "ridge-and-valley" zone, while the actual thickness is around 20 nm according to the lowest point on the height profile (**Figures S4C and D**).

S2.5 Elemental composition by XPS

The atomic composition of the PA shells of the CSPCs is listed in table S2. The relatively high oxygen concentration on the PA shell surface, especially the one fabricated with 2% MPD, is probably due to the oxidation of the precursor MPD molecules during the prolonged absorption process before the interfacial polymerization. The primary chemical shift is most likely attributed to the elements directly bonded to the carbon atom of interest, and the secondary shift (β-shift) is attributed to the strong electron withdrawing groups (amide and carboxylic acid) bonded to the carbon atom [3]. To quantify the bonding state of the atoms of interest, peak deconvolution was performed using CasaXPS software. The C1s peaks of the membranes were deconvoluted into five peaks at 284.8 eV (C-C, C=C, and C-H), 285.5 eV (β-shift for C-CONH, C-COO), 286.1 eV (C-N), 288.1 eV (N-C=O), and 289.0 eV (O-C=O). The narrow spectrum of O1s confirmed the amount of amide bond at 532.0 eV (N-C=O) and the unreacted acyl chloride group of TMC hydrolyzed to the carboxylic acid group at 533.2 eV (O-C=O). The amide bond at 400.0 eV (N-

C=O) was found in the N1s spectrum with a small amount of unreacted amine at 401.5 eV (R-$N^{+}H_3$) (**Figure S5 and Table S3**).

S2.6 Mechanical tests of the flat-sheet hydrogel-based PA membranes

To investigate the mechanical properties of hydrogel-based PA membranes, flat-sheet hydrogel-based PA membranes were chosen to perform the wrinkling and cracking based tests, due to the curved nature of the spherical membranes (PA shells) making the above mechanical tests impossible. Considering the thickness and roughness similarity to the PA shells, flat-sheet PA membranes synthesized using only hexane as the organic phase during interfacial polymerization were chosen as the samples (see S2.3). The thickness and roughness of the PA membrane samples were listed in the table below:

PA Membrane-TMC in pure hexane (wt% amine)	Interface type	Thickness from AFM (nm)	RMS[a] roughness R_{rms} (nm)
2% MPD	Flat	178.0 ± 7.2	95.2 ± 3.5
1% MPD	Flat	97.0 ± 13.2	51.3 ± 4.3
0.5% MPD	Flat	17.9 ± 0.4	15.0 ± 0.8
0.1% MPD	Flat	12.9 ± 0.2	0.8 ± 0.1

[a]RMS stands for root mean square.

Under compressive stress, the thin film placed on elastic substrate wrinkles and forms a well-defined wave pattern, the elastic modulus of the thin film can be estimated based on Equation (S1) [3-5],

$$E_m = 3E_s \frac{1-v_{nf}^2}{1-v_s^2}\left(\frac{\lambda}{2\pi h_m}\right)^3 \quad (S1)$$

where, E and v are the elastic modulus and the Poisson's ratio, respectively, with the subscripts s and m standing for substrate and membrane. The wavelength is annotated as λ. Membrane thickness is annotated as h_m.

PDMS (1.2 - 1.6 mm thick) was used as the substrate for the wrinkling test, which was fabricated by casting the mixed solution of Sylgard 184 (base:curing agent, mass ratio, 10:1) onto a glass slide and cured at 75ºC for 2 hours. The tensile test was performed by a universal test machine on the PDMS stripes. The elastic modulus of PDMS (1.64 ± 0.14 MPa) was obtained from the linear elastic region (less than 1% strain). The Poisson's ratio of PDMS and polyamide membrane was assumed to be 0.49 and 0.39, respectively [3]. To perform the wrinkling tests, the PDMS stripes of 20×15 mm^2 dimension was first stretched up to 10% strain using a 3D printed and assembled stretching tool (**Figure S6A**). The synthesized PA membrane floating on the water was then transferred onto the PDMS substrate and dried. After totally dried, the PDMS stripe was gently recovered back to its original length by turning the screw reversely, which applied a compressive stress on the top PA membrane to form the wave pattern (**Figure S6B**). Subsequently, the as-prepared samples were analyzed by AFM for the wavelength measurements (**Figure S6C**).

The supplementary mechanical properties, including onset fracture strain and fracture strength, were estimated based on the theory that the average fragment width, $\langle d \rangle$, is inversely proportional to the strain. Thus, based on the average width of fragments, both the properties above can be obtained from Equation (S2),

$$\langle d \rangle = \frac{2h_m\sigma^*}{E_s\varepsilon'} \quad (S2)$$

where σ* is the fracture strength, and ε' equals strain ε minus onset strain ε*. The cracking test was performed by stretching the PDMS-PA membrane composite using the stretching tool to form cracks on the membrane. The evolution of the average fragment width along the strain was observed and recorded by an optical microscope (**Figure S7A**). From the results, we can tell that the smooth membranes synthesized with low MPD concentration were more rigid and stiff than

the highly crumpled ones synthesized with higher MPD concentrations. The superior mechanical endurance of the smooth membrane is most likely attributed to the dense and isotropic structure [6].

S2.7 Multiphysics modeling of the swelling of the hydrogel sphere

The swelling of the hydrogel is a coupled process involving large deformation of the hydrogel network and mass transport of the absorbents, in this case, water molecules. From thermodynamics perspective, the swelling represents a process of hydrogel-water system entropy increasing caused by the decrease of the chemical energy embedded in the polymer chains, which is well depicted by the Flory-Rehner free energy function [7]. The free energy of the swelling hydrogel network consists two parts, the entropy of network stretching and the entropy of the mixing of network polymer and water molecules, which governs the displacement/deformation of the network and water mass transfer, respectively [8-10].

Given that, we simulated the initial transient swelling of the hydrogel sphere based on the model developed by Lucantonio et al. [11]. The deformation of the gel is depicted by the deformation gradient $\boldsymbol{F}$, which is related to the gradient of the displacement $\boldsymbol{u}$ by $\boldsymbol{F} = \boldsymbol{I} + \nabla \boldsymbol{u}$. Here $\boldsymbol{I}$ is the identity matrix. The determinant of $\boldsymbol{F}$, J, here equals λ^3, where λ represents the stretch. For the swelling of a hydrogel from the reference state, the following volume constraint holds [11],

$$J = \frac{1}{J_0} + \Omega c \quad (S3)$$

where J_0 represents the volume deformation from the dry state to the reference state, Ω is the solvent molar volume, which is 6.023×10^{-5} $m^3 \cdot mol^{-1}$ for water, and c is the molar concentration of the solvent in the hydrogel. The conservative equations based on the force and mass balance as follows should also be satisfied,

$$div\, \boldsymbol{S} = 0 \quad (S4)$$

$$\frac{dc}{dt} = -div\,\boldsymbol{h} \quad (S5)$$

where $\boldsymbol{S}$ is the first Piola-Kirchhoff stress and $\boldsymbol{h}$ is the water mass flux.

To derive the constitutive equations in supplementary to the conservative equations, the Flory-Rehner free energy density per unit of gel volume, referred to as ϕ was written as [12],

$$\phi = \frac{1}{2}G(\boldsymbol{FF_0} \cdot \boldsymbol{FF_0} - 3) + \frac{RT}{\Omega}H \quad (S6)$$

where $\boldsymbol{F_0} = \lambda_0\boldsymbol{I}$, and $\boldsymbol{A} \cdot \boldsymbol{B}$ denotes the inner product between two second order tensors $\{\boldsymbol{A}, \boldsymbol{B}\}$; G is the shear modulus taking the value of 40 kPa in this model [11], and H represents the mixing entropy taking the form,

$$H = \Omega c ln\left(\frac{\Omega c}{1+\Omega c}\right) + \chi\frac{\Omega c}{1+\Omega c} \quad (S7)$$

where χ represents the dimensionless measure of the enthalpy of mixing, which takes the value of 0.2 in this model [11]. Based on the free energy function, the constitutive relations are determined as,

$$\boldsymbol{S} = \frac{\partial\phi}{\partial\boldsymbol{F}} - p\boldsymbol{F}^* = \frac{G}{\lambda_0}\boldsymbol{F} - p\boldsymbol{F}^* \quad (S8)$$

$$\mu = \frac{\partial\phi}{\partial c} + p\Omega = RT\left(\ln\left(\frac{\Omega J_0 c}{1+\Omega J_0 c}\right) + \frac{1}{1+\Omega J_0 c} + \frac{\chi}{(1+\Omega J_0 c)^2}\right) + \Omega p \quad (S9)$$

$$\boldsymbol{h} = -\frac{cD}{RT}\nabla\mu \quad (S10)$$

where $\boldsymbol{F}^{*} = J\boldsymbol{F}^{-T}$; p is a Lagrange multiplier representing a pressure field remained unknown in the model; μ is the chemical potential of the solvent; D is the diffusivity of the solvent, which is 8×10^{-10} $m^2\cdot s^{-1}$ for water.

Eventually, the model was implemented in COMSOL Multiphysics software to find a displacement $\boldsymbol{u}$ and a solvent concentration c to satisfy the conservative Equations (S4)-(S5), the constitutive Equations (S8)-(S10), and the volume constraint Equation (S3) under appropriate initial and boundary conditions.

S2.8 Three-dimensional (3D) filtration experiments

After shrinking in a 2 M KCl solution for over 90 min, the CSPC was transferred into 1 ml feed solution to initiate the swelling. The size of the swelling CSPC was monitored by an optical microscope (**Figure S10**). The volume of the CSPC was calculated based on the radius measured by a circle measuring tool in the microscope software. The water absorption rate was calculated based on the changing volume of the sphere over time. After 45 min of water absorption, the ion concentration in the residual solution was measured by atomic absorption spectroscopy (AAS). The salt rejection was calculated based on Equation (S11):

$$Salt\ rejection = \left(1 - \frac{C_0 * V_0 - C_t * (V_0 - V')}{C_0 * V'}\right) * 100\% \quad (S11)$$

where C_0 represents the ion concentration of the stock feed solution; C_t represents the ion concentration of the residual solution at time t; V_0 is the feed volume, 1 ml; V' represents the volume of the absorbed water, which equals the volume of the CSPC at time t (V_{Ct}) minus the initial volume of the CSPC (V_{C0}).

For the water filtration experiments in bivalent ion solutions, the cation concentration was 35 mM equivalent to the Na^+ concentration in 2 $g \cdot l^{-1}$ NaCl. The swelling ratio (end volume/initial volume) was controlled at 9 equivalent to that in the tests conducted in 2 $g \cdot l^{-1}$ NaCl.

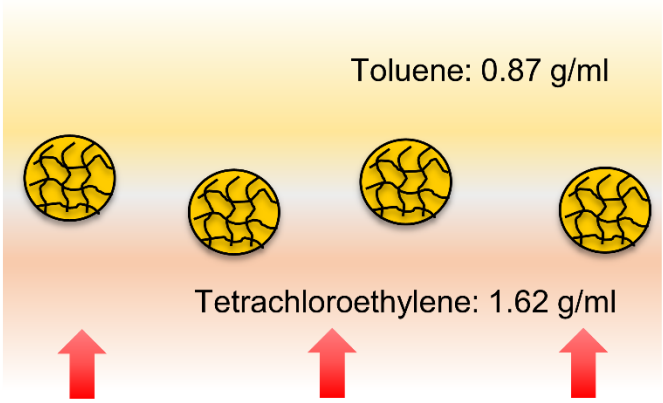

Fig. S1. Schematic showing the spherical core suspension polymerization.

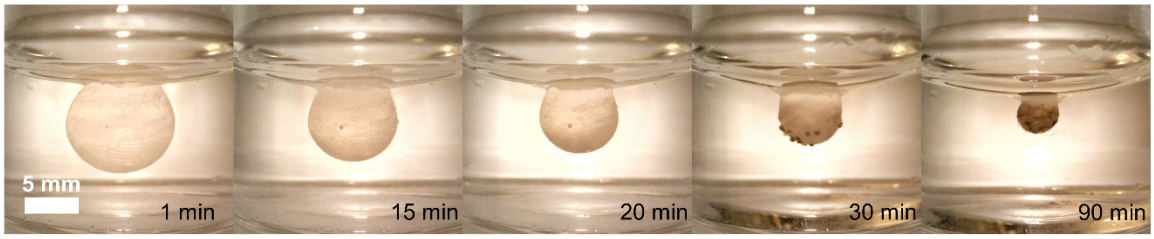

Fig. S2. Photographs showing the shrinking of the CSPC.

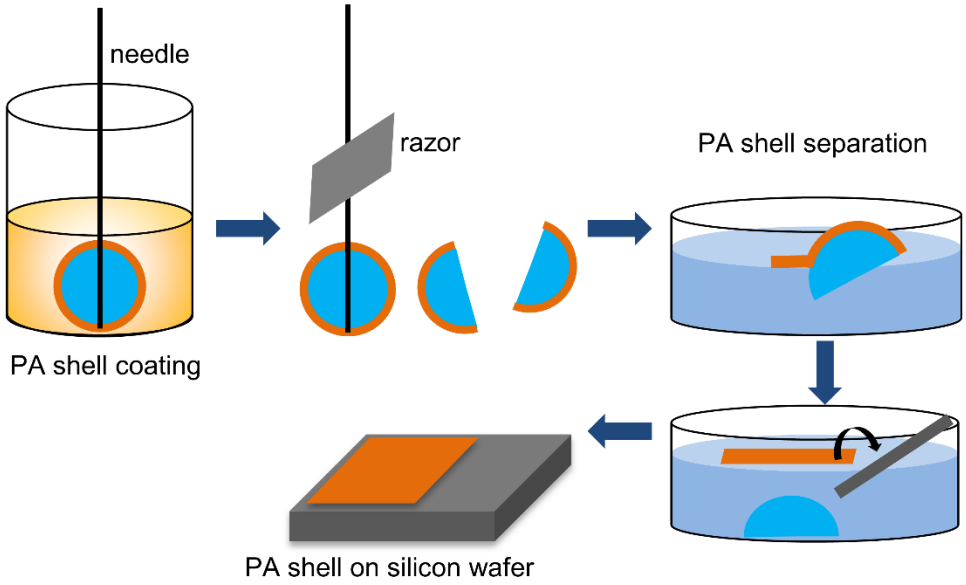

Fig. S3. Schematics showing the PA shell separation and transfer process.

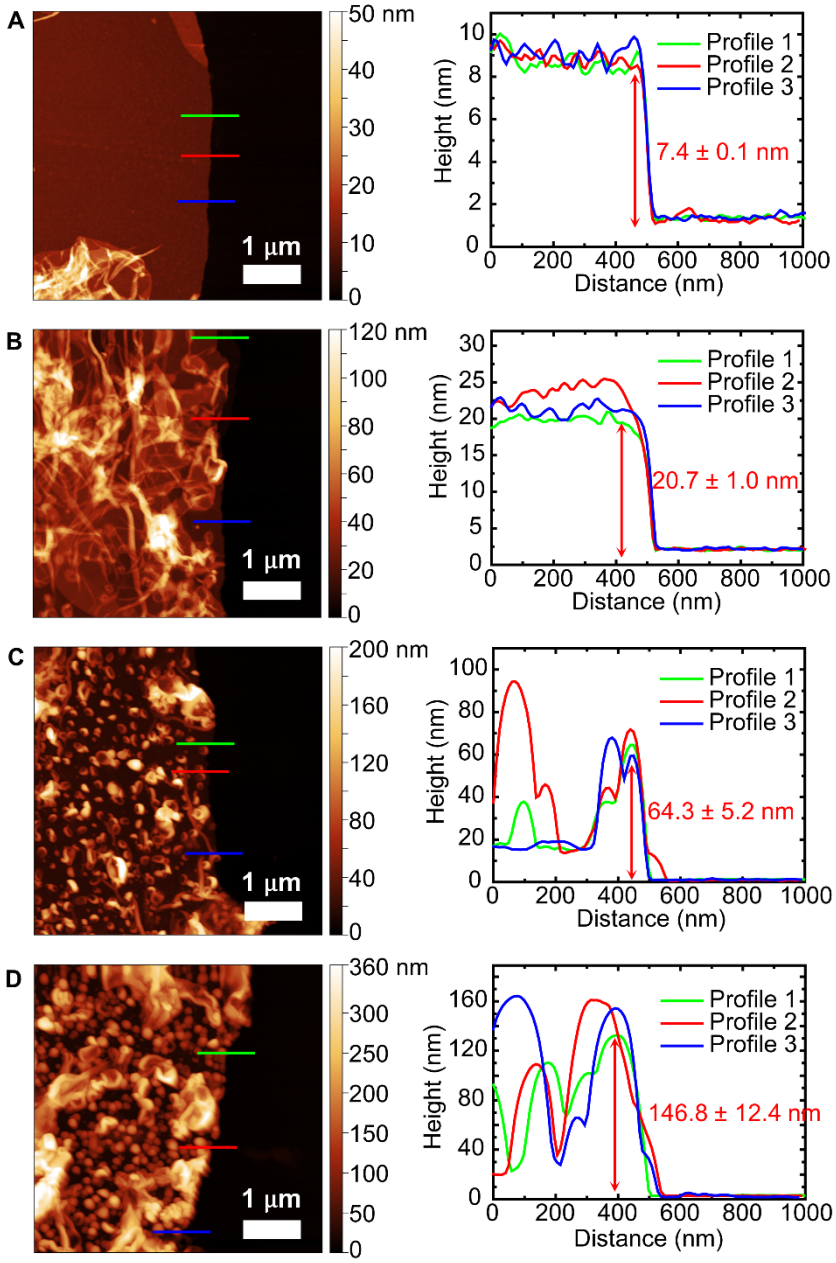

Fig. S4. Thickness quantification of the PA shells by AFM. Left**,** AFM images showing the PA shell made from 0.1% MPD (**A**), 0.5% MPD (**B**), 1.0% MPD (**C**), and 2% MPD (**D**) on the silicon substrate, respectively. Right, height profiles. The lines in the AFM images represent the positions where height profiles were taken.

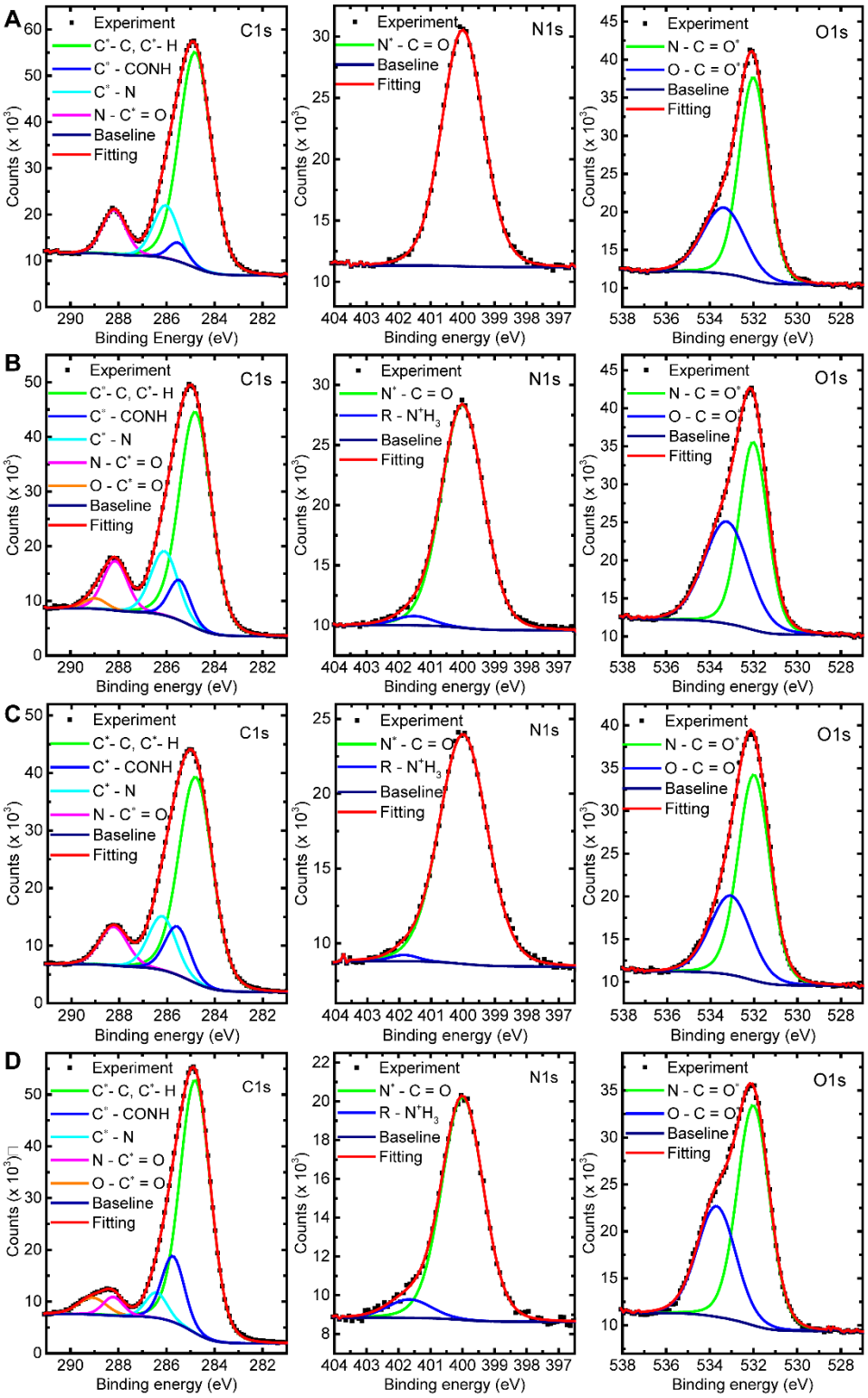

Fig. S5. XPS narrow spectrums of the PA shells. The PA shells made from 0.1% MPD (**A**), 0.5% MPD (**B**), 1.0% MPD (**C**), and 2.0% MPD (**D**).

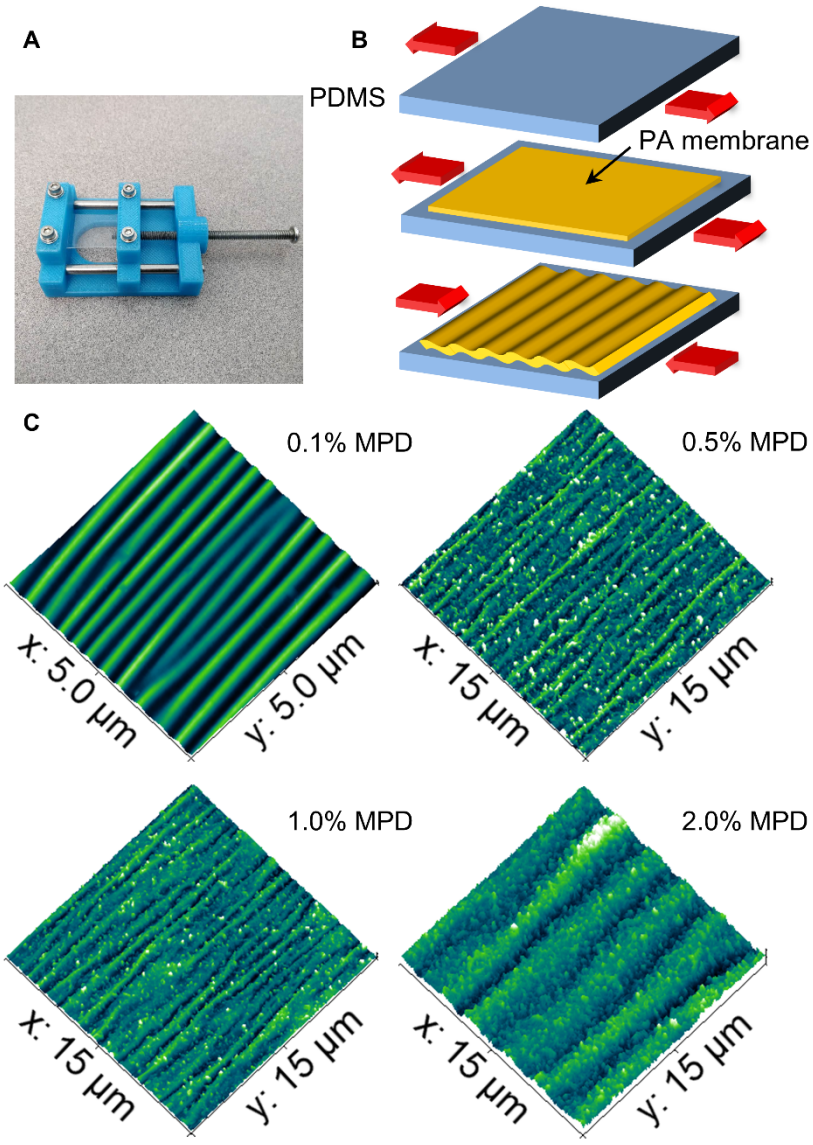

Fig. S6. Wrinkling test of the PA membranes. A, 3D printed stretching tool. **B**, Schematics showing the wave forming process. **C**, AFM measurements of the as-prepared wrinkled PA membranes (wt% amine). The mean wavelength was estimated from at least 15 wavelengths.

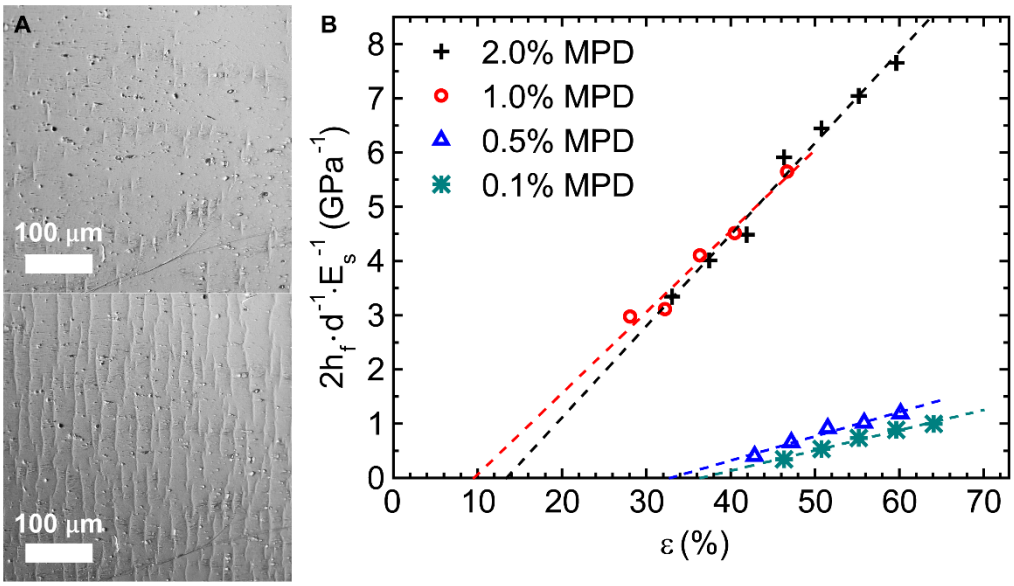

C

PA membrane (wt% amine)	E_m (MPa)	Fracture onset strain ε^* (%)	Fracture strength σ^* (MPa)
2.0% MPD	60.66	13.41	49.38
1.0% MPD	26.04	9.57	56.94
0.5% MPD	1056.66	32.82	223.07
0.1% MPD	689.21	36.44	274.72

Fig. S7. Cracking test of the PA membranes. A, The optical microscope images showing the cracks of 1.0% MPD membrane formed at 28.1% strain (upper image) and 46.7% strain (bottom image). **B**, The plots of rescaled crack density versus the strain for PA membranes of different thicknesses. The dashed lines represent the linear fitting of the measured data to the strain-dependent crack density model Equation (S11), from which the intercept (ε^*) and the slope ($1/\sigma^*$) were derived. **C**, Summary of the results.

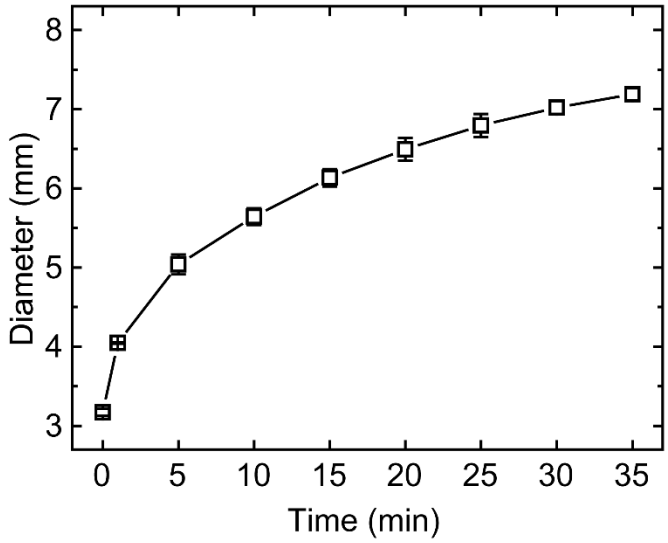

Fig. S8. The diameter of the CSPC plotted against the swelling time in DI water. Error bars represent the standard deviations from 3 independent experiments.

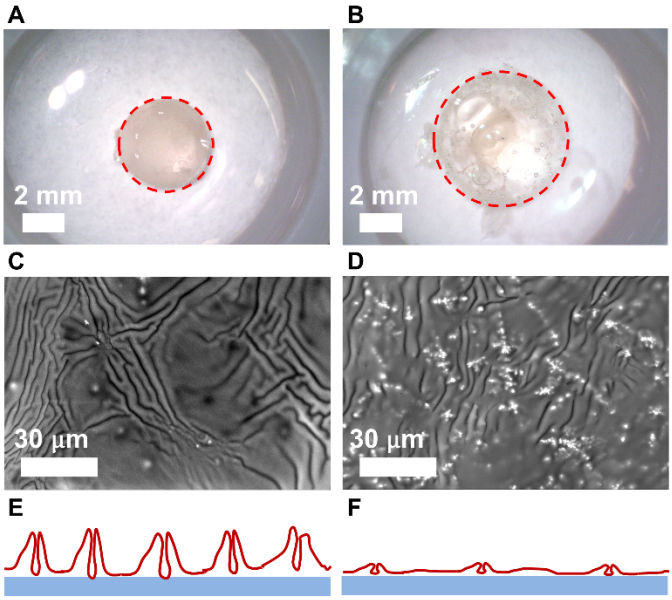

Fig. S9. Swelling behaviour of CSPC1. A and **B**, Photographs of the swelling CSPC1 at the diameter of ~4 mm (**A**) and ~6 mm (**B**). The CSPC1 diameter was quantified based on the circle radius (red dashed circle). **C** and **D**, ESEM images showing the PA shell on the swelling CSPC1 at the diameter of ~4 mm (**C**) and ~6 mm (**D**). **E** and **F**, Sketches representing the profiles of folds of big amplitude (**E**) and folds of small amplitude (**F**).

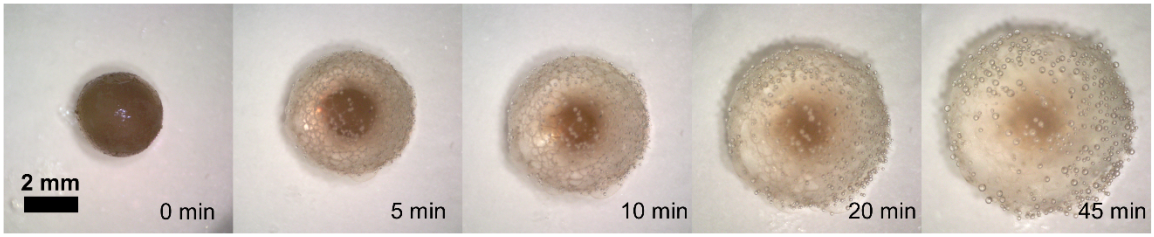

Fig. S10. Photographs showing the swelling of the CSPC (1.0% MPD) in 2 g·l^{-1} NaCl solution.

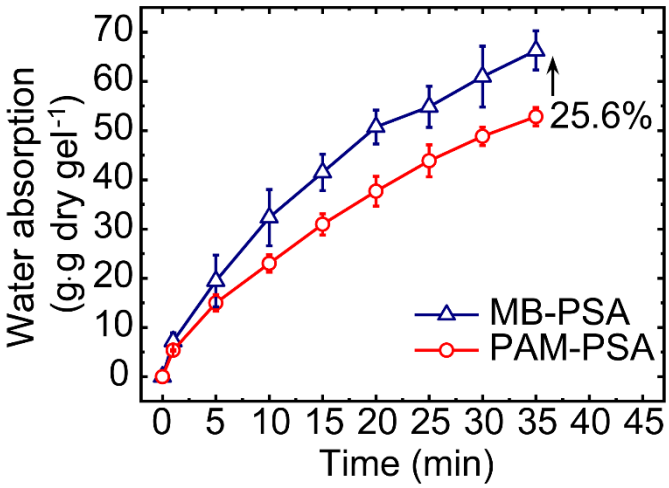

Fig. S11. Comparison between the swellings of the maize bran (MB)-PSA based CSPC and the PAM-PSA based CSPC in DI water. Error bars represent the standard deviations from 3 independent experiments.

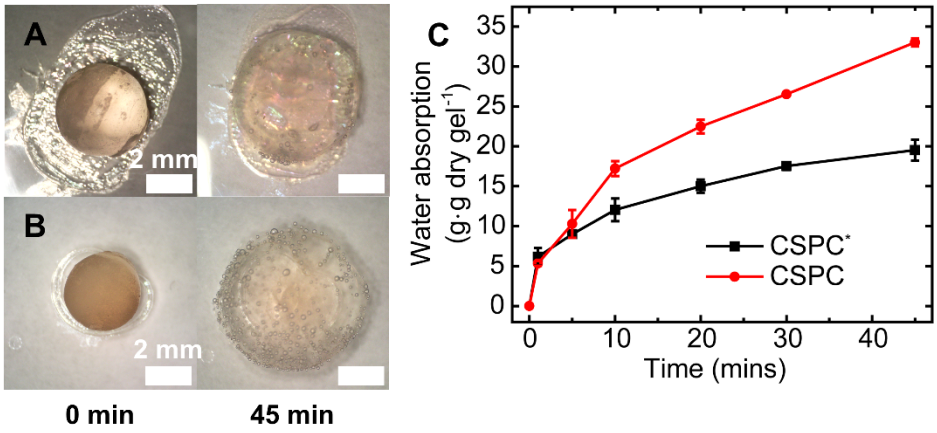

Fig. S12. Swelling capacity of the CSPCs of intact and impaired PA shells. a, The CSPC* (0.1% MPD) with an impaired shell (showed no salt rejection) before (left) and after (right) swelling; **b**, The CSPC (0.1% MPD) with an intact shell (100% salt rejection) before (left) and after (right) swelling. **c**, The water absorption of the both CSPCs plotted against swelling time. Error bars represent the standard deviations calculated from 3 independent experiments.

Table S1. Roughness of PA membranes synthesized under different conditions.

PA membrane (wt% amine)	RMS[a] roughness R_{rms} (nm)
2% MPD	66.5 ± 11.8[b]
1% MPD	42.7 ± 6.2
0.5% MPD	14.4 ± 0.3
0.1% MPD	0.4 ± 0.03

[a]RMS stands for root mean square.
[b]Standard deviations were calculated from results of at least three areas of each membrane sample. Samples were prepared in triplicates for each reaction condition.

Table S2. Atomic composition of the PA shells from the CSPCs.

PA shells (wt% amine)	C%	N%	O%
2.0% MPD	72.0 ± 1.8[a]	8.6 ± 0.2	19.4 ± 2.0
1.0% MPD	70.4 ± 0.2	12.3 ± 0.5	17.2 ± 0.3
0.5% MPD	69.2 ± 0.1	13.0 ± 0.2	17.7 ± 0.2
0.1% MPD	72.1 ± 0.5	12.6 ± 0.2	15.3 ± 0.2

[a]Standard deviations were calculated from the results of two different areas on each sample.

Table S3. Deconvolution and composition of the XPS narrow spectrums of the PA shells of the CSPCs.

PA shell (wt% amine)	C1s			O1s			N1s		
	Energy (eV)	Species	(%)	Energy (eV)	Species	(%)	Energy (eV)	Species	(%)
2.0% MPD	284.8[a]	C-H, C-C, C=C	72.6						
	285.7	C-CONH, C-COO	14.1	532.0	N-C=O	62.6	400.0	N-C=O	92.0
	286.4	C-N	5.2	533.7	O-C-O	37.4	401.7	$R\text{-}N^{+}H_3$	8.0
	288.2	N-C=O	3.6						
	289.1	O-C=O	4.5						
1.0% MPD	284.8	C-H, C-C, C=C	64.9						
	285.6	C-CONH, C-COO	11.2	532.0	N-C=O	66.8	400.0	N-C=O	98.5
	286.2	C-N	13.9	533.1	O-C-O	33.2	401.9	$R\text{-}N^{+}H_3$	1.5
	288.2	N-C=O	10.0						
0.5% MPD	284.8	C-H, C-C, C=C	63.0						
	285.5	C-CONH, C-COO	7.9	532.0	N-C=O	54.1	400.0	N-C=O	96.4
	286.1	C-N	15.9	533.2	O-C-O	46.0	401.5	$R\text{-}N^{+}H_3$	3.6
	288.1	N-C=O	11.1						
	289.0	O-C=O	2.1						
0.1% MPD	284.8	C-H, C-C, C=C	71.6						
	285.5	C-CONH, C-COO	3.8	532.0	N-C=O	67.6	400.0	N-C=O	100
	286.0	C-N	13.8	533.4	O-C-O	32.4			
	288.2	N-C=O	10.9						

[a]Binding energies have a deviation of ± 0.2 eV.

Table S4. Summary of 3D filtration performance of all the CSPCs.

CSPC (PA shell wt% amine)	2 g·l^{-1} NaCl		4 g·l^{-1} NaCl		6 g·l^{-1} NaCl	
	Salt rejection (%)	Average water absorption (g·g dry gel^{-1})	Salt rejection (%)	Average water absorption (g·g dry gel^{-1})	Salt rejection (%)	Average water absorption (g·g dry gel^{-1})
2.0% MPD	97.3 ± 1.1[a]	42.8 ± 1.5	71.7 ± 0.0	41.4 ± 0.8	62.0 ± 2.4	30.9 ± 1.1
1.0% MPD	99.8 ± 0.4	41.5 ± 2.1	72.4 ± 6.7	44.3 ± 1.8	79.1 ± 6.6	34.4 ± 0.2
0.5% MPD	86.9 ± 0.1	40.6 ± 0.5	80.1 ± 8.6	34.3 ± 0.8	94.0 ± 4.5	22.7 ± 0.9
0.1% MPD	100 ± 0.0	33.0 ± 0.5	ND[b]	ND	ND	ND

[a]Standard deviations were calculated based on 3 independent experiments.
[b]ND stands for not determined.

S3. References

1. M. Zhang, Z. Cheng, T. Zhao, M. Liu, M. Hu and J. Li, *Journal of agricultural and food chemistry*, 2014, **62**, 8867-8874.
2. N. Y. Yip, A. Tiraferri, W. A. Phillip, J. D. Schiffman and M. Elimelech, *Environmental Science & Technology*, 2010, **44**, 3812-3818.
3. S. Karan, Z. Jiang and A. G. Livingston, *Science*, 2015, **348**, 1347-1351.
4. C. M. Stafford, C. Harrison, K. L. Beers, A. Karim, E. J. Amis, M. R. VanLandingham, H.-C. Kim, W. Volksen, R. D. Miller and E. E. Simonyi, *Nature Materials*, 2004, **3**, 545-550.
5. J. Y. Chung, J.-H. Lee, K. L. Beers and C. M. Stafford, *Nano Letters*, 2011, **11**, 3361-3365.
6. F. Foglia, S. Karan, M. Nania, Z. Jiang, A. E. Porter, R. Barker, A. G. Livingston and J. T. Cabral, *Advanced Functional Materials*, 2017, **27**, 1701738.
7. P. J. Flory and J. R. Jr., *The Journal of Chemical Physics*, 1943, **11**, 521-526.
8. W. Hong, X. Zhao, J. Zhou and Z. Suo, *Journal of the Mechanics and Physics of Solids*, 2008, **56**, 1779-1793.
9. W. Hong, Z. Liu and Z. Suo, *International Journal of Solids and Structures*, 2009, **46**, 3282-3289.
10. M. L. Huggins, *The Journal of Chemical Physics*, 1941, **9**, 440-440.
11. A. Lucantonio, P. Nardinocchi and L. Teresi, *Journal of the Mechanics and Physics of Solids*, 2013, **61**, 205-218.
12. M. Doi, *Journal of the Physical Society of Japan*, 2009, **78**, 052001.